Estimate of Turbulent Energy Dissipation Rate from the VHF Radar And Radiosonde Observations in the Antarctic

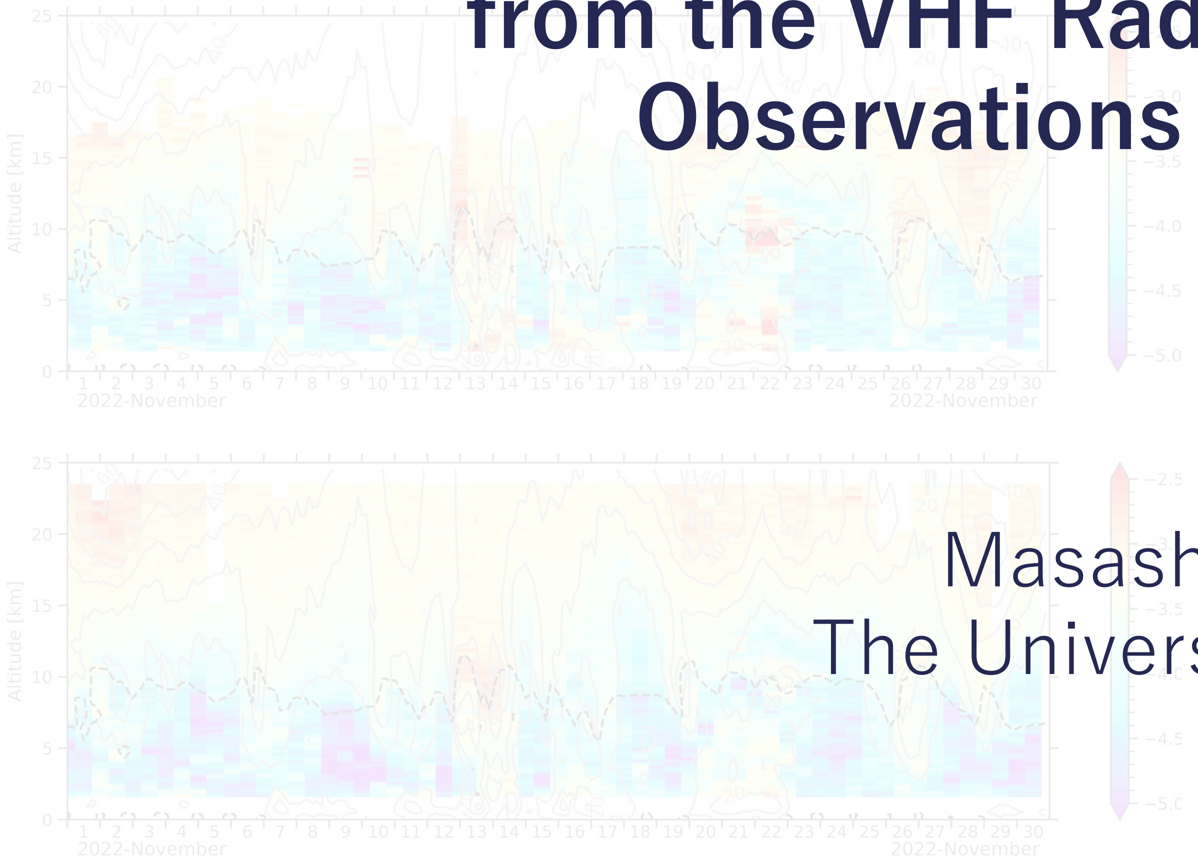

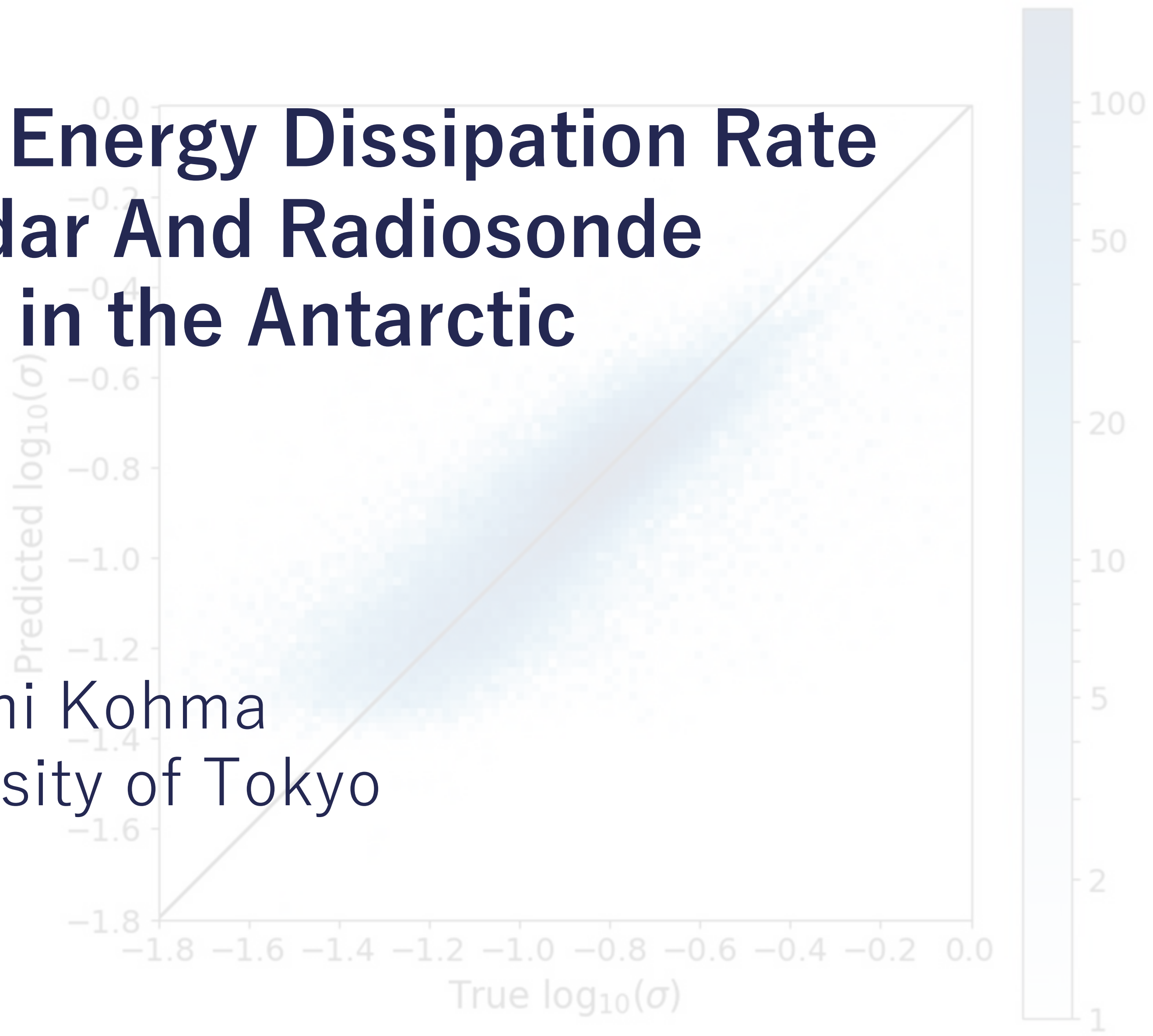

Masashi Kohma
The University of Tokyo

This study is supported by JST FOREST program

Outline

0. Introduction
    - Estimation of energy dissipation rates in the free atmosphere

1. Turbulent Energy Dissipation Rates (ε) Comparison:
    - Used VHF radar data at Syowa Station, Antarctic
    - Compared with radiosonde-based estimation via Thorpe method

(Kohma et al., 2019)

2. Preliminary Results of Machine Learning (ML) Approach for Estimating ε
    - Developed a ML-based algorithm to estimate ε from the radiosonde observations.

Introduction

- **Turbulent kinetic energy dissipation rates** (ε):
  A variable representing loss rate of turbulent kinetic energy

- Estimation method of ε in the free atmosphere
  - VHF/UHF radar (e.g., Sato & Woodman, 1982; Hocking, 1983)
    - **Spectral width method** / Power method
  - **Radiosondes** (e.g., Clayson & Kantha, 2008; Wilson et al., 2011)
    - **Thorpe method**
  - Aircraft/UAV (e.g., Sharman et al., 2014; Luce et al., 2018; 2023)
  - Rocket (e.g., Luebken, 1997; Luebken et al., 2002)

  etc. (e.g., Schneider et al., 2015)

Introduction

Estimation of ε by Thorpe method (Thorpe, 1977)

Thorpe Scale L_{T} : Local overturning length scale

1. Sort the measured density profile (left panel) into a monotonic profile (right panel)
2. Calculate displacement distance of each sample ($d = z_m - z_n$)
3. Obtain L_{T} as the root-mean-square of d

Ozmidov Scale $L_{\mathrm{O}} \equiv \left(\frac{\varepsilon}{N^3}\right)^{1/2}$: Maximum turbulence length scale in a stratified fluid

Oceanic microstructure observations empirically indicated the proportional relation

$$L_{\mathrm{O}} = cL_{\mathrm{T}}.\ (c = 0.25\text{—}4)$$

Using this relation, we obtain

$$\boxed{\varepsilon = c^2 L_{\mathrm{T}}^2 N^3}$$

Measured density profile　　Sorted density profile

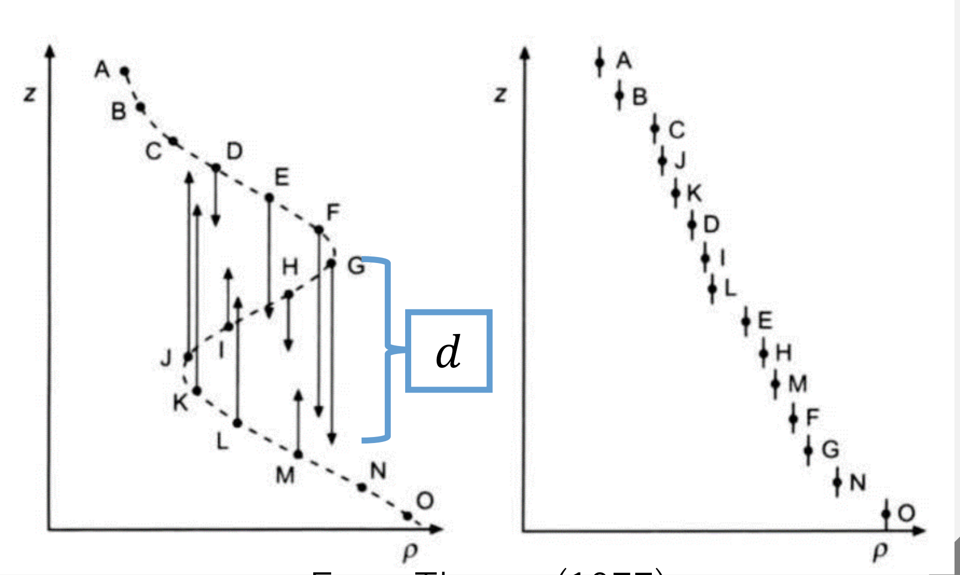

From Thorpe (1977)

Introduction

Uncertainty of ε from Thorpe method

- The uncertainty of c (0.25-4) results in two orders of magnitude uncertainty of ε ($\because \varepsilon \propto c^2$)
- Fritts et al. (2016): $\mathbf{c}$ values can vary depending on event type (e.g., KH instability or wave breaking) and timing
- Schneider et al. (2015): The discrepancy of ε for individual layers is up to a factor of 3000.

⇒ Comparison between **radar-based** and **Thorpe-based ε** using observations at Syowa Station, Antarctic (Kohma et al., 2019)

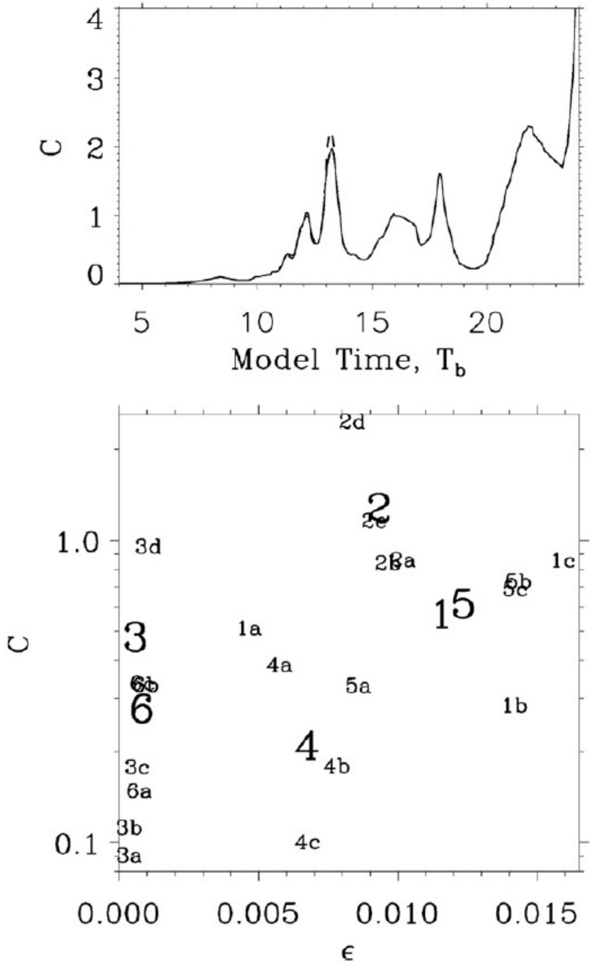

Fritts et al. (2016)

PANSY

The program of Antarctic Syowa radar (PANSY radar)

Mesosphere-Stratosphere-Troposphere/Incoherent Scatter radar at Syowa Station (69S, 40E) in the Antarctic

System	Pulse Doppler radar. Active phased array system
Center freq.	47MHz
Antenna	Array consisting of 1045 crossed Yagi antennas equivalent to the circular area with a diameter of 160m (18000m^2), light and tough (12.6kg/antenna)
Transmitter	1045 solid-state TR modules Peak Power : 520kW
Receiver	55 channel digital receiving systems Ability of imaging and interferometry obs
Power consumption	66kW (E-class amplifier)
Peripheral	24 antennas for E-layer FAI observation

Previous studies using the radar

- GWs in the troposphere-stratosphere:
  (Sato et al., 2014; Minamihara et al. 2018; 2020)
- GWs in the mesosphere:
  (Sato et al., 2017; Shibuya et al., 2017; Shibuya & Sato, 2019)
- Turbulent energy dissipation rates:
  (Kohma et al., 2019; 2020; 2021; Minamihara et al., 2023)

Observation of 3-d wind vectors in height regions of 1.5-20km and 60-90 km, and plasma parameters in 100-500 km with fine resolution and high accuracy

Direct estimation of vertical flux of horizontal momentum associated with gravity waves

The full-system observations with all antenna groups has been operated continuously since October 2015.

Data: PANSY radar

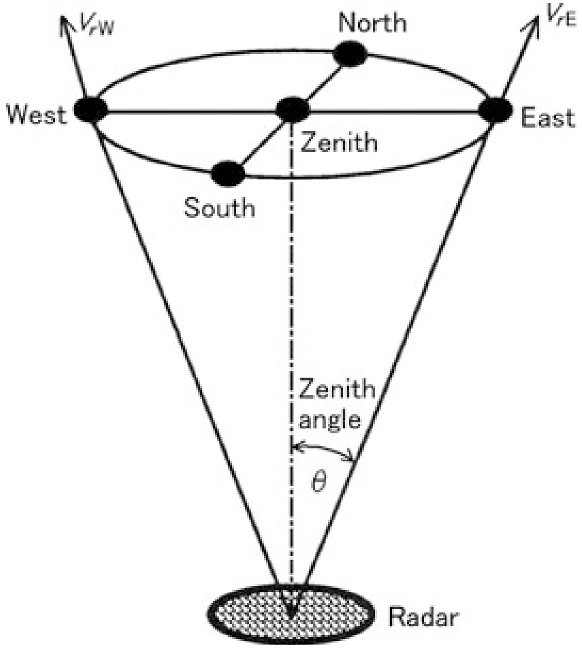

Time interval: ~200 s
Range resolution: 150 m (troposphere and stratosphere)

For estimation of energy dissipation rates,
4 off-vertical beams with a zenith angle of 10°
are used to avoid the effect of specular reflection.

Estimation of ε from radar spectral widths

- $\sigma_{\mathrm{obs}}^2 = \sigma_{\mathrm{T}}^2 + \sigma_{\mathrm{B}}^2 + \sigma_{\mathrm{S}}^2 + \sigma_{\mathrm{W}}^2$ (σ_T^2: Turbulence; σ_B^2: Beam broadening; σ_S^2: Shear broadening; σ_W^2: Time broadening)

  Beam broadening σ_{B}^2 is removed using an algorithm developed by Nishimura et al. (2020)

- $\boxed{\varepsilon = 0.46 N w_{\mathrm{std}}^2}$ $\left(w_{\mathrm{std}}^2 = \frac{\sigma_{\mathrm{T}}^2}{2\ln 2}\right)$ (Sato & Woodman 1982; Hocking, 1983)

  where N is buoyancy frequency

  In the following, ε averaged over 4 off-vertical beams are shown.

Comparison of ε - radar estimation and Thorpe estimation

$c(\equiv L_o/L_T) = 1$

Radar estimates ε_R Thorpe estimates ε_T

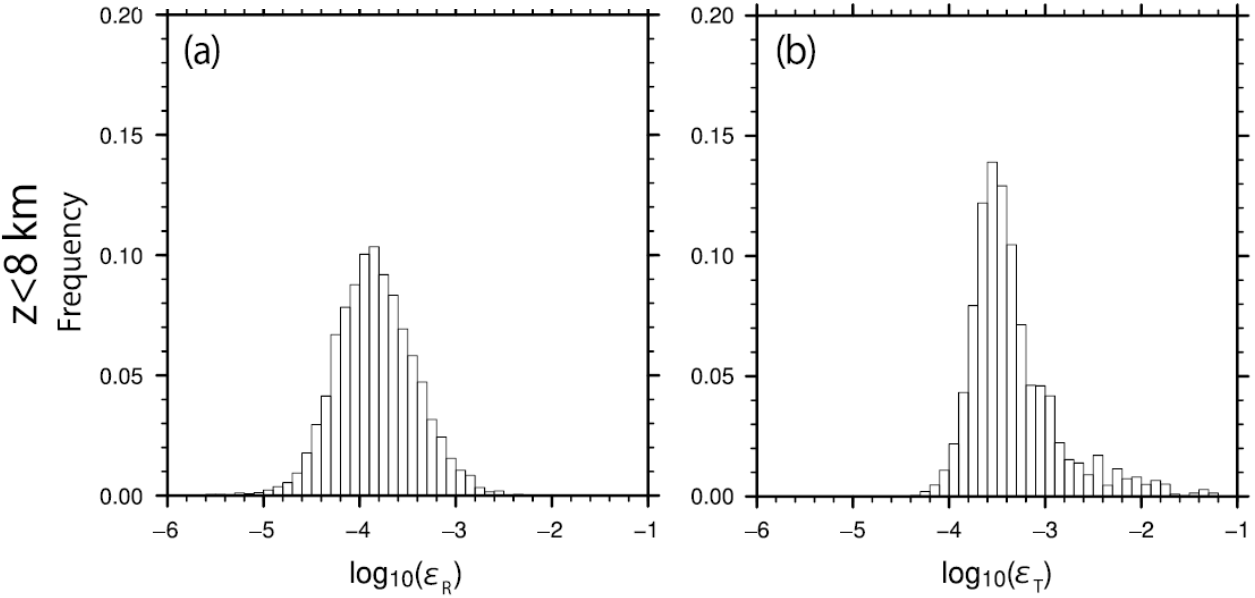

Vertical profiles of median values of ε in 2016

$\varepsilon_R/\varepsilon_T$

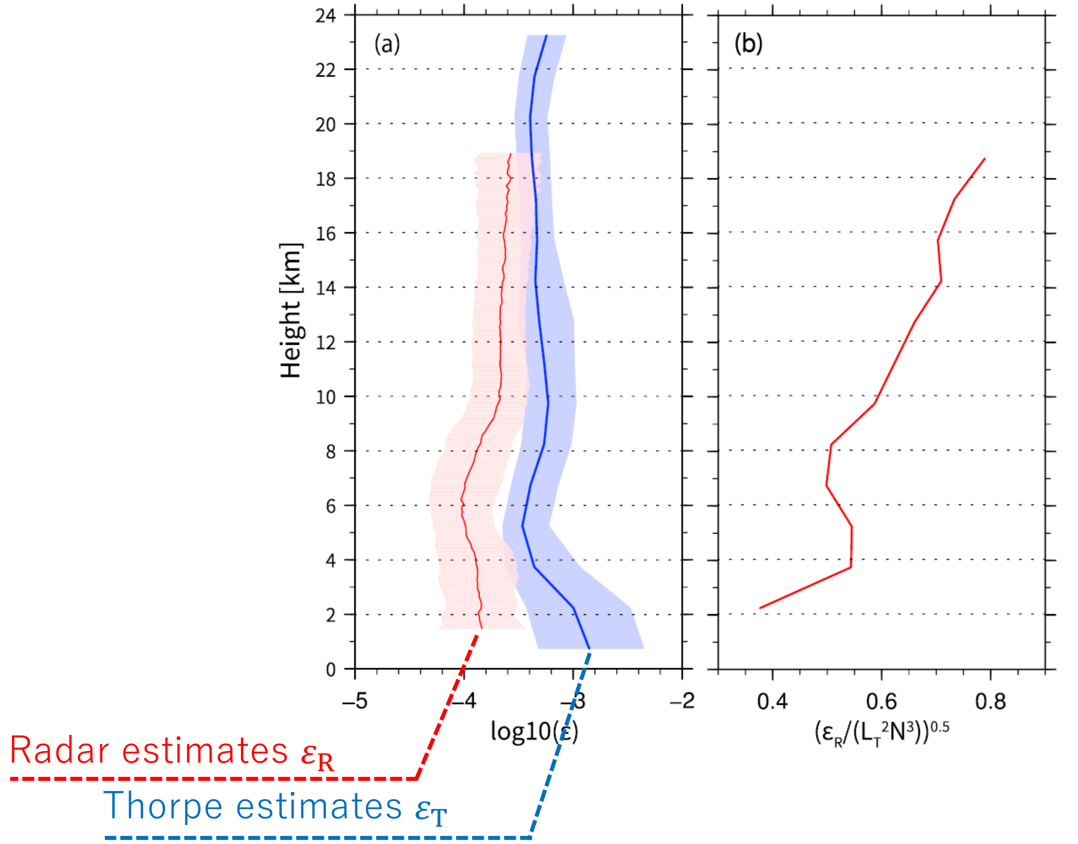

The ratio of radar-based ε to Thorpe-based ε is small in z=1.5–9 km compared to over 11 km.

There are more recent studies including discussion on ε estimation based on Thorpe method. (e.g., Wang et al., 2019; Luce et al., 2023)

Short-term variation of ε from the radar
- A time-height section (Sep. 2017)

$\log_{10}(\varepsilon)$ (color), Tropopause (PV=2PVU, black broken contour), $\sqrt{u^2+v^2}$ (JRA55, gray contour)

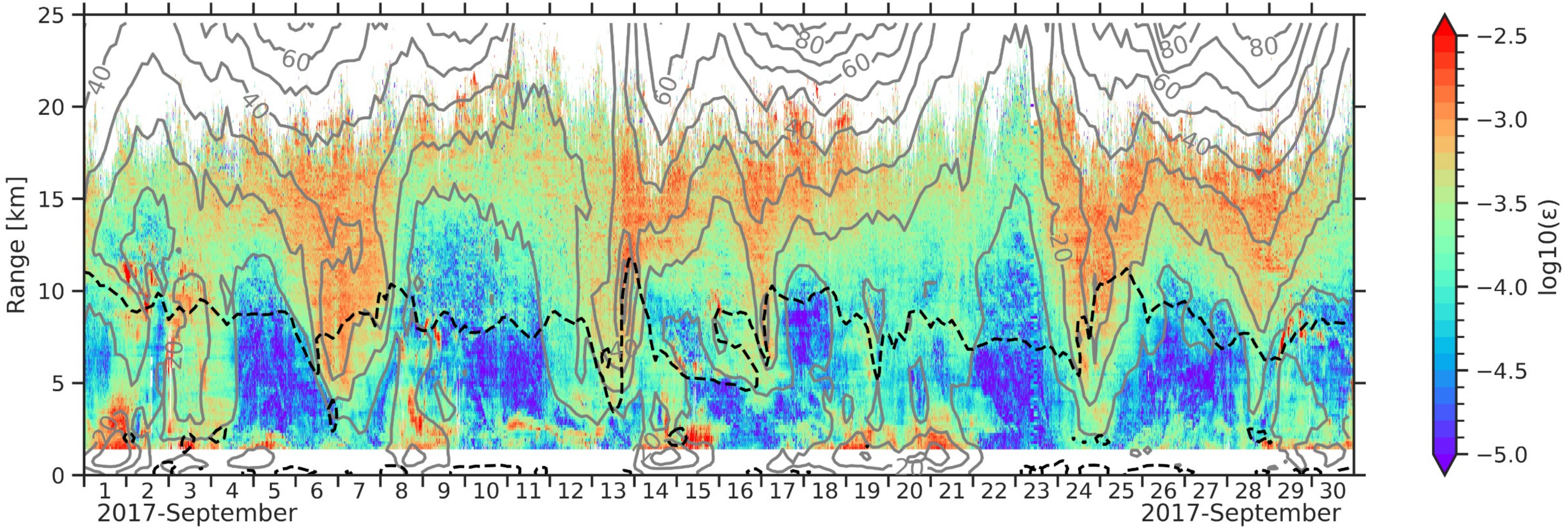

Short-term variation of ε from the radar - A time-height section (Sep. 2017)

$\log_{10}(\varepsilon)$ (color), Tropopause (PV=2PVU, black broken contour), $\sqrt{u^2+v^2}$ (JRA55, gray contour)

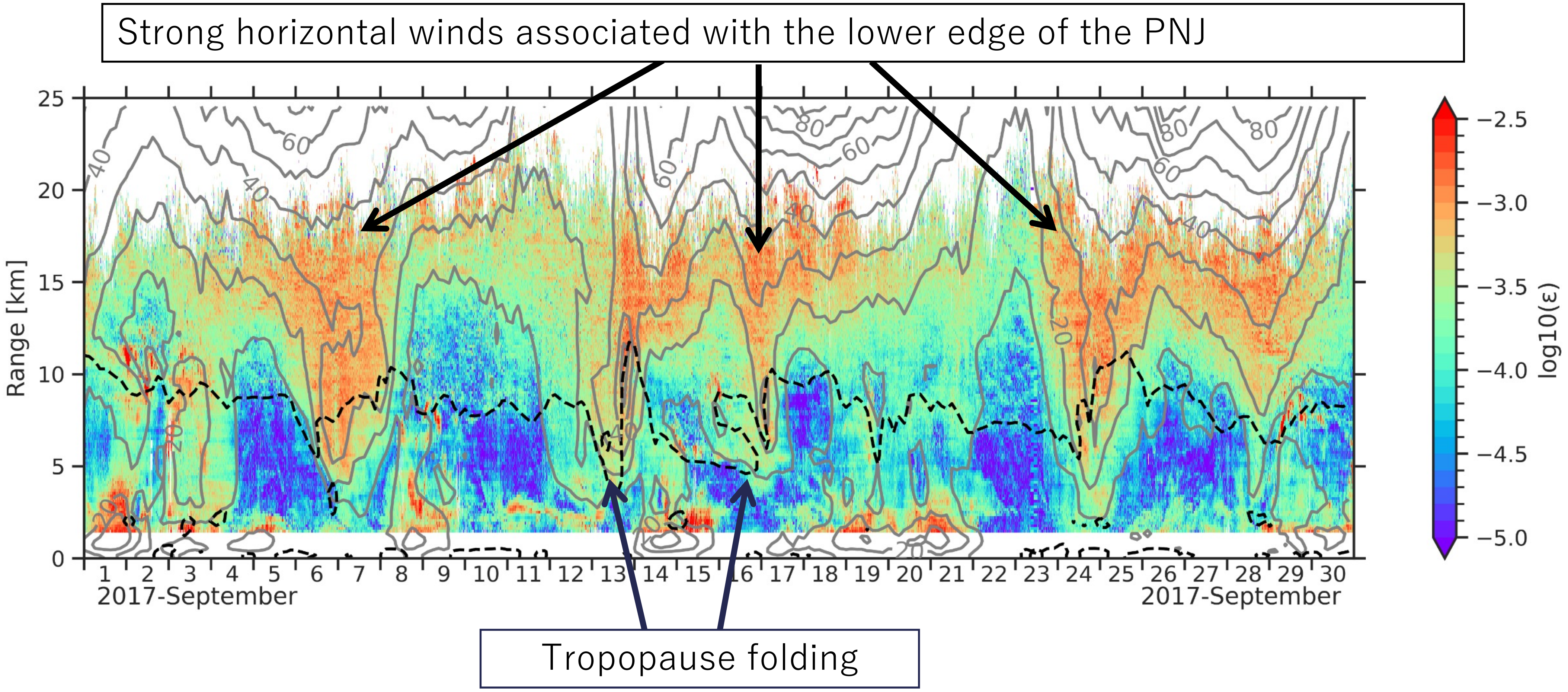

Note: Tropopause folding occur frequently along the coast of Antarctica compared to the southern mid latitudes (Kohma et al., 2022)

Short-term variation of ε from the radar - A time-height section (Sep. 2017)

$\log_{10}(\varepsilon)$ (color), Tropopause (PV=2PVU, black broken contour), $\sqrt{u^2+v^2}$ (JRA55, gray contour)

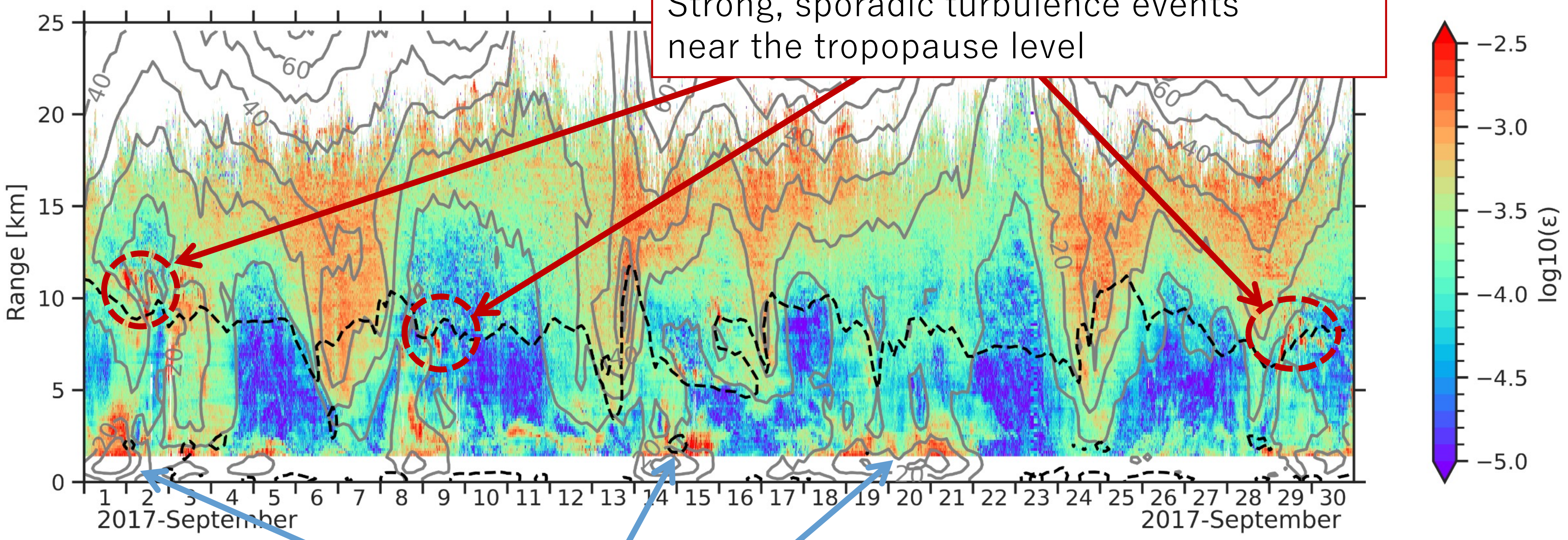

Strong, sporadic turbulence events near the tropopause level

Strong surface winds associated with synoptic-scale disturbances

K-H billows observed by PANSY radar

- Minamihara et al. (2023)
  - Kelvin-Helmholtz (K-H) billow using Frequency-domain Interferometric Imaging (FII) techniques
    - FII mode： dt=～13 s, dz=～9.4 m
    - Standard mode： dt=～90 s, dz=～150 m
  - From 10-day observation period, about 70 K-H billows are detected

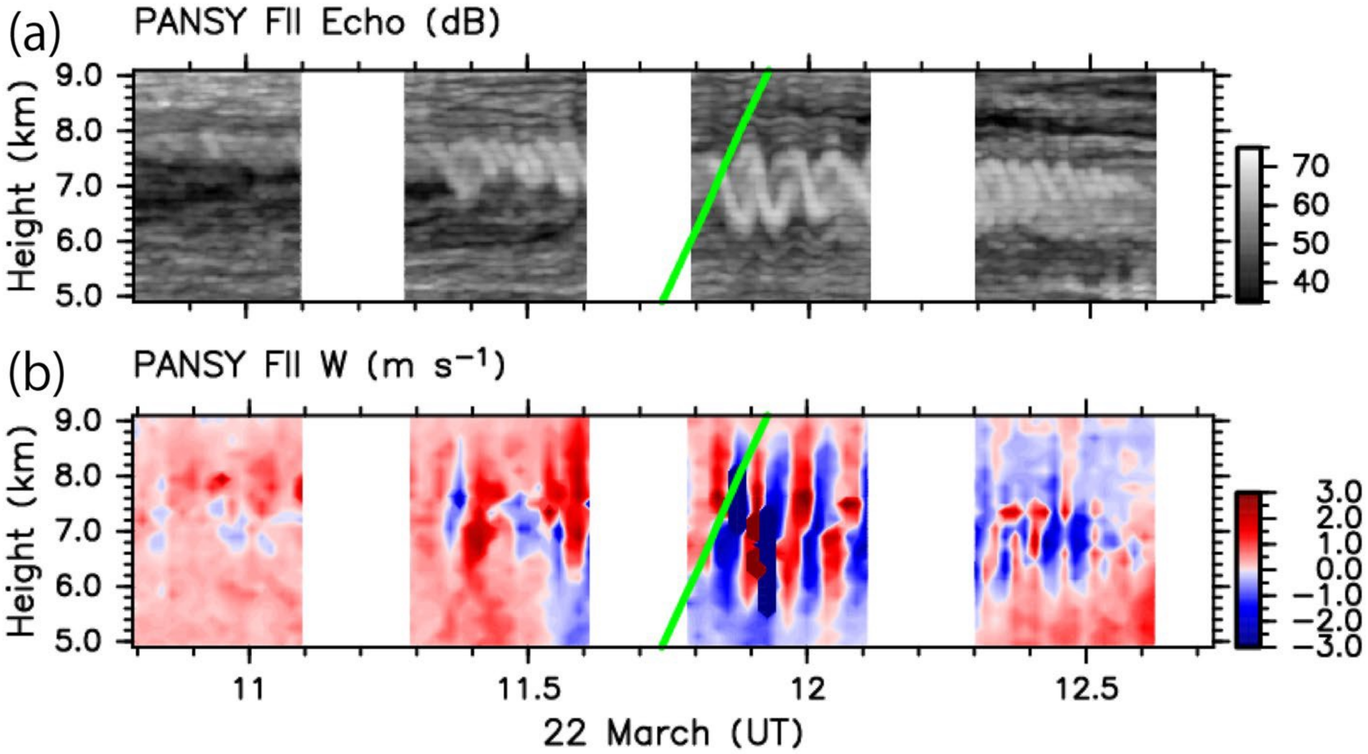

An approach of estimation of turbulent energy dissipation rates from radiosonde observations based on machine learning

Preliminary results

Motivation

Radar-based estimates:

Traditionally used
Fine temporal resolution

Limitation:
Limited availability of radar observation sites

Radiosonde-based estimates:

Extensive radiosonde observation network

Limitation:
Uncertainty of ε estimates

Syowa Station, Antarctic

Numerous simultaneous observations of a VHF radar and radiosondes since October 2015

Purpose of the study:

Estimate $f(\boldsymbol{x}_{\mathrm{sonde}})$ s.t.

$$f(u_{\mathrm{sonde}}, v_{\mathrm{sonde}}, \theta_{\mathrm{sonde}}) = \varepsilon_{\mathrm{radar}}$$

using machine learning(ML) approach based on a dataset of simultaneous observations of a radar and radiosondes.

In this presentation,
the preliminary results of ML-based approach for estimating ε is shown.

So far, we have NOT addressed

- Applicability to other sites (i.e., mid latitudes & tropics)
- Effect of processes related to latent heat release

Data: Radiosondes

Operational radiosonde observations at Syowa Station

- Meisei RS-06G/RS-11G, twice a day (00UT, 12UT)
- Processed data (NOT Raw data)
- u, v, & θ
  - Relative humidity (RH) is not used in the following results.
- From Oct. 2015 to Dec. 2022
- Interpolated at a constant vertical interval of 5 m from data with $\Delta t = 1$ sec.
- Restricted observations where horizontal distance between the radar and radiosondes < 25 km

Data: PANSY radar

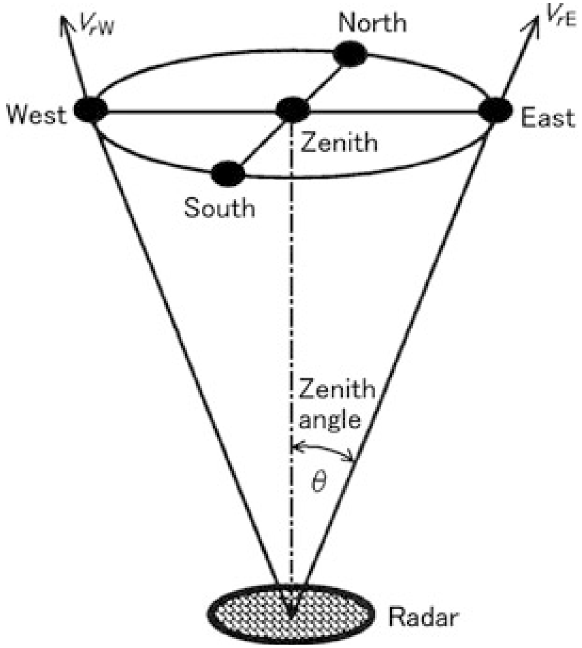

Time interval: ~200 s
Range resolution: 150 m

4 oblique beams with a zenith angle of 10°
are used to avoid the effect of specular reflection.

Estimation of ε from radar spectral width

- $\sigma_{\mathrm{obs}}^2 = \sigma_{\mathrm{T}}^2 + \sigma_{\mathrm{B}}^2 + \sigma_{\mathrm{S}}^2 + \sigma_{\mathrm{W}}^2$ (σ_T^2: Turbulence; σ_B^2: Beam broadening; σ_S^2: Shear broadening; σ_W^2: Time broadening)

  Beam broadening σ_{B}^2 is removed using an algorithm developed by Nishimura et al. (2020)

- $\boxed{\varepsilon = 0.46 N w_{\mathrm{std}}^2}$ $\left(w_{\mathrm{std}}^2 = \frac{\sigma_{\mathrm{T}}^2}{2 \ln 2}\right)$ (Sato & Woodman 1982; Hocking, 1983)

  In the following, w_{std} averaged over 4 oblique beams are shown.

w_{std} (standard deviation of vertical wind fluctuations due to turbulence) is used for the ML-based approach

Training dataset: $\{\widehat{w_{\rm std}}(z_i)\}$, $\left\{[\hat{u}(z), \hat{v}(z), \theta'(z)]_{z_i-1.5\rm km}^{z_i+1.5\rm km}\right\}$

Radar: $w_{\rm std}(z_i)$

- Temporal average: until 1 h after radiosonde launch
  - Yeo-Johnson transformation

$$\widehat{w_{\rm std}} = \begin{cases} \left((w_{\rm std}+1)^{\lambda}-1\right)/\lambda & \text{if } \lambda \neq 0, w_{\rm std} \geq 0 \\ \ln(w_{\rm std}+1) & \text{if } \lambda = 0, w_{\rm std} \geq 0 \\ -\left((-w_{\rm std}+1)^{2-\lambda}-1\right)/(2-\lambda) & \text{if } \lambda \neq 0, w_{\rm std} < 0 \\ -\ln(-w_{\rm std}+1) & \text{if } \lambda = 0, w_{\rm std} < 0 \end{cases}$$

For making the $w_{\rm std}$ distribution approximate normal distribution

Radiosondes: u, v, θ $(z = [z_i - 1.5\rm km, z_i + 1.5\rm km])$

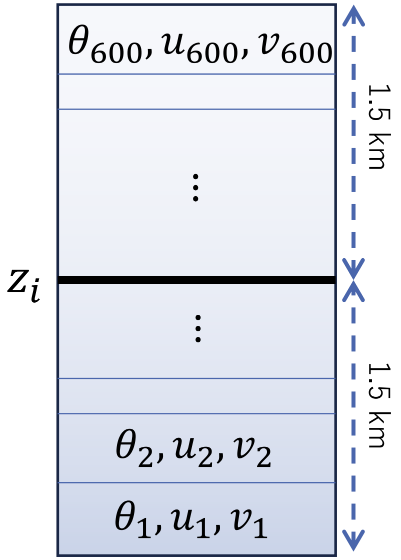

- Data dimension:
  3 km [600 x (u, v, θ)]
- $\theta' = \theta - \bar{\theta}$
  ($\bar{\theta}$: Vertical average over 3 km)
- $(\hat{u}, \hat{v})^{\rm T} = \mathbf{R}(u, v)^{\rm T}$

$$\mathbf{R} = \begin{pmatrix} \cos\varphi & -\sin\varphi \\ \sin\varphi & \cos\varphi \end{pmatrix} \quad (0 < \varphi < 2\pi)$$

Rotation angle φ is given randomly for each profile

✓ Data augmentation technique for improving the ML model's generalization ability

Training data: October 2015 - December 2021

Validation data: January - December 2022

Validation data is NOT used during the training process but is utilized for the validation purposes.

Machine Learning (ML) model

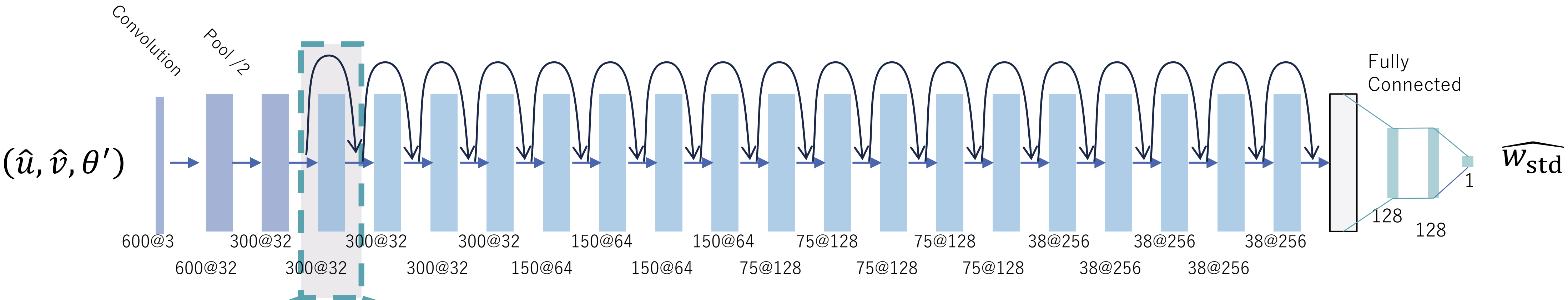

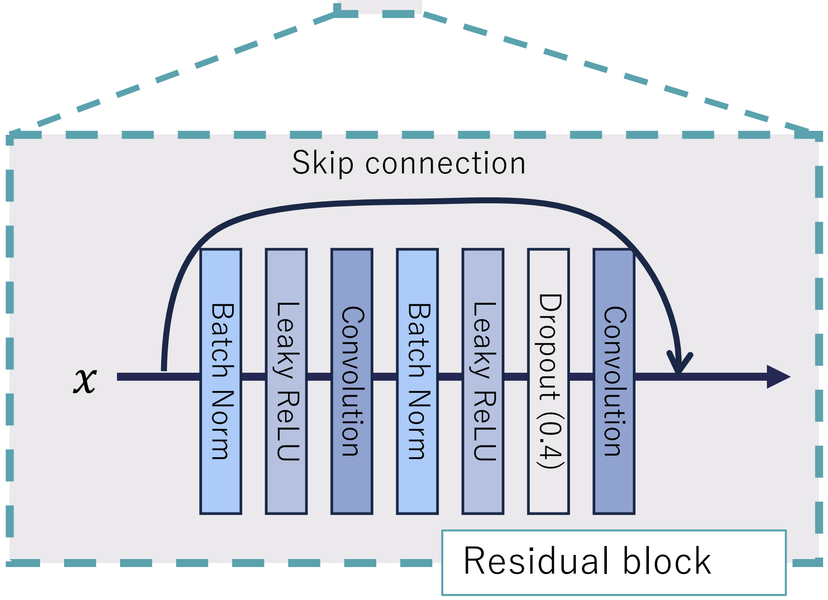

- Number of parameters: ~3,470,000
- Loss function: Mean square error
- Optimization: Adaptive Moment Estimation
  (learning rate: 0.001)
- Mini batch size: 512

cf. Residual Neural Network (ResNet; He et al., 2015)

ResNet enables the model with hundreds of layers to train easily and approach better accuracy when the model is going deeper

Results: Radar observation vs. ML prediction

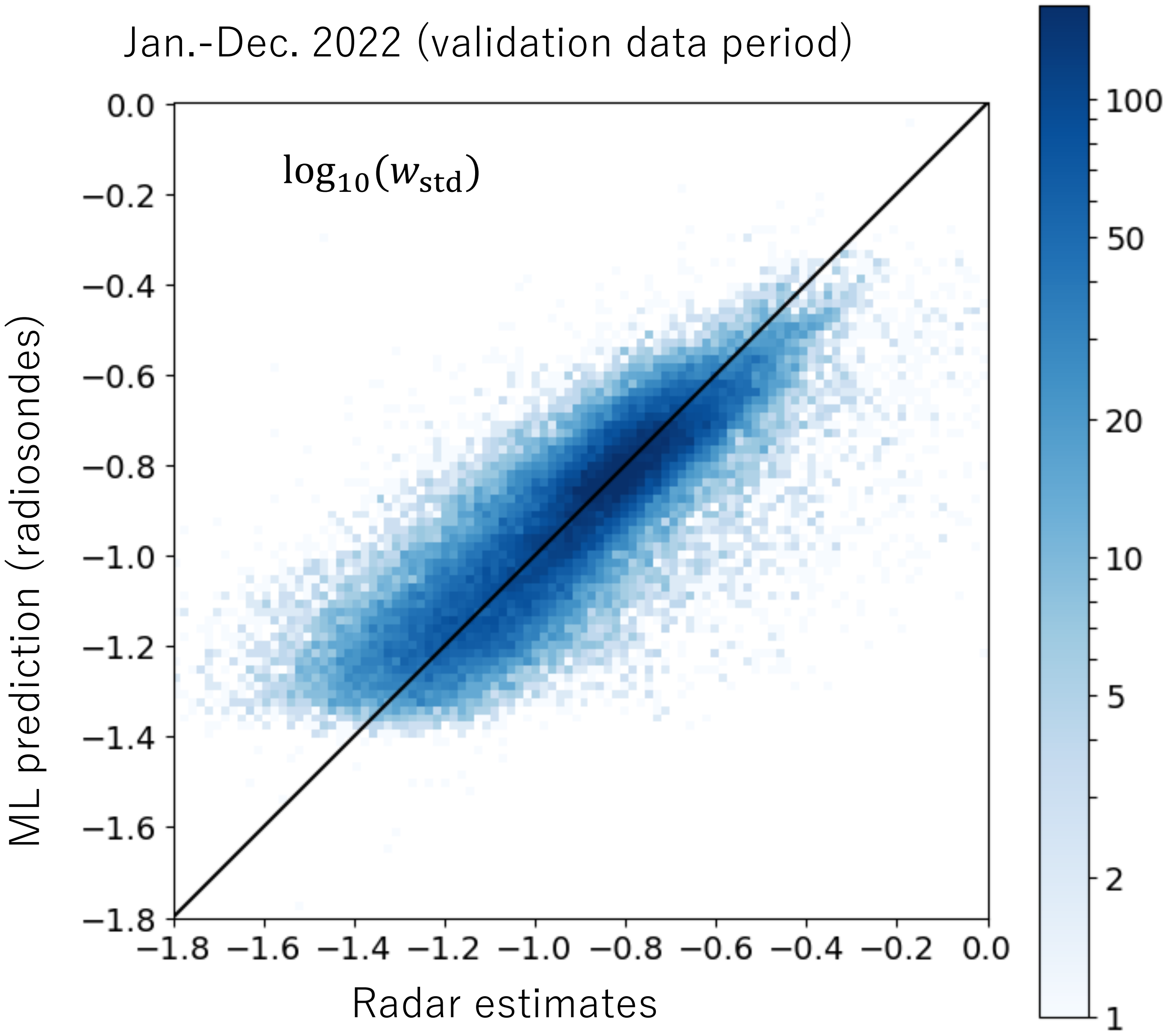

NOTE: Observations in 2022 are not used in the training process

Results: Time-height section of ε in November 2022

ε from the radar (dt=12h)

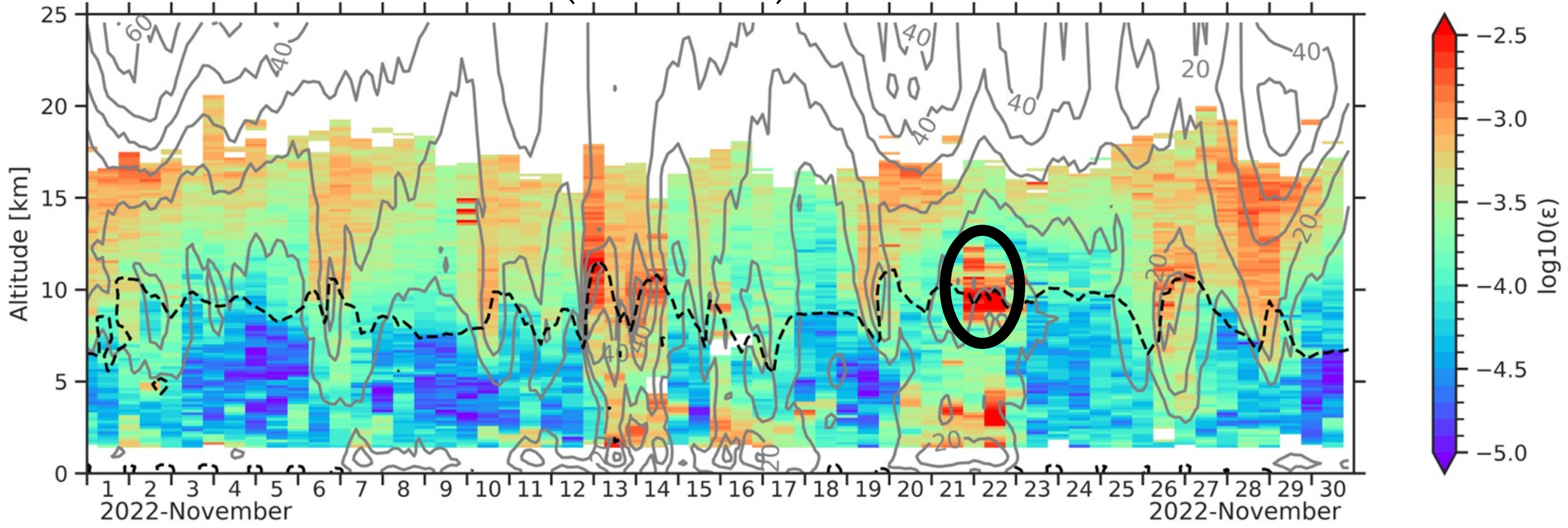

ε from ML-based prediction (radiosondes)

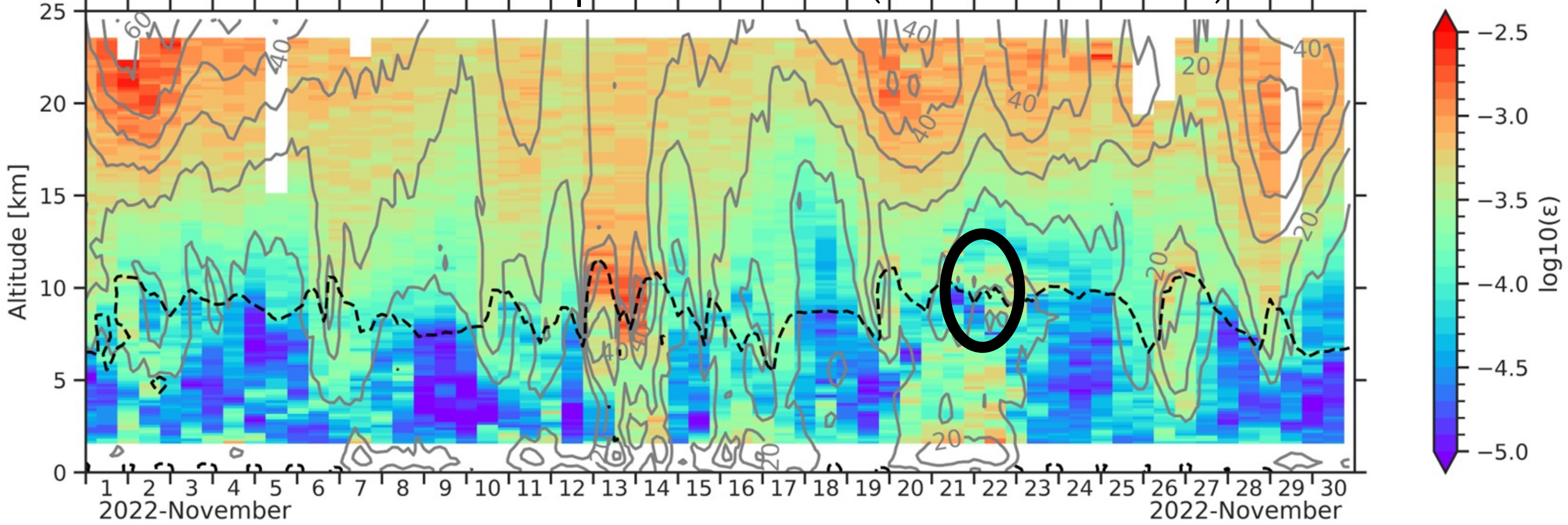

Successful case s

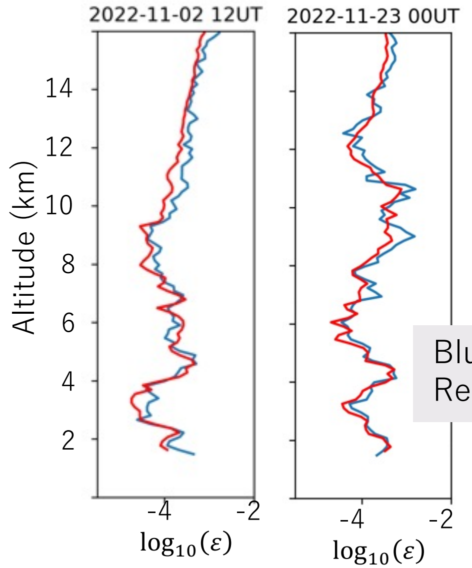

Blue: Radar
Red: ML

Missing large ε

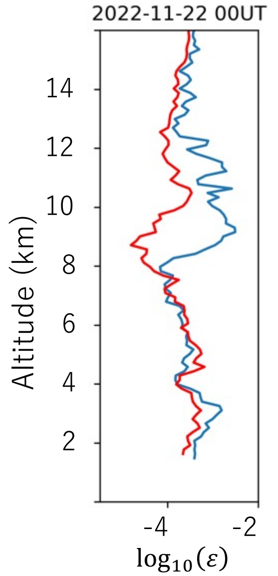

Results: Annual mean & monthly mean ε in 2022

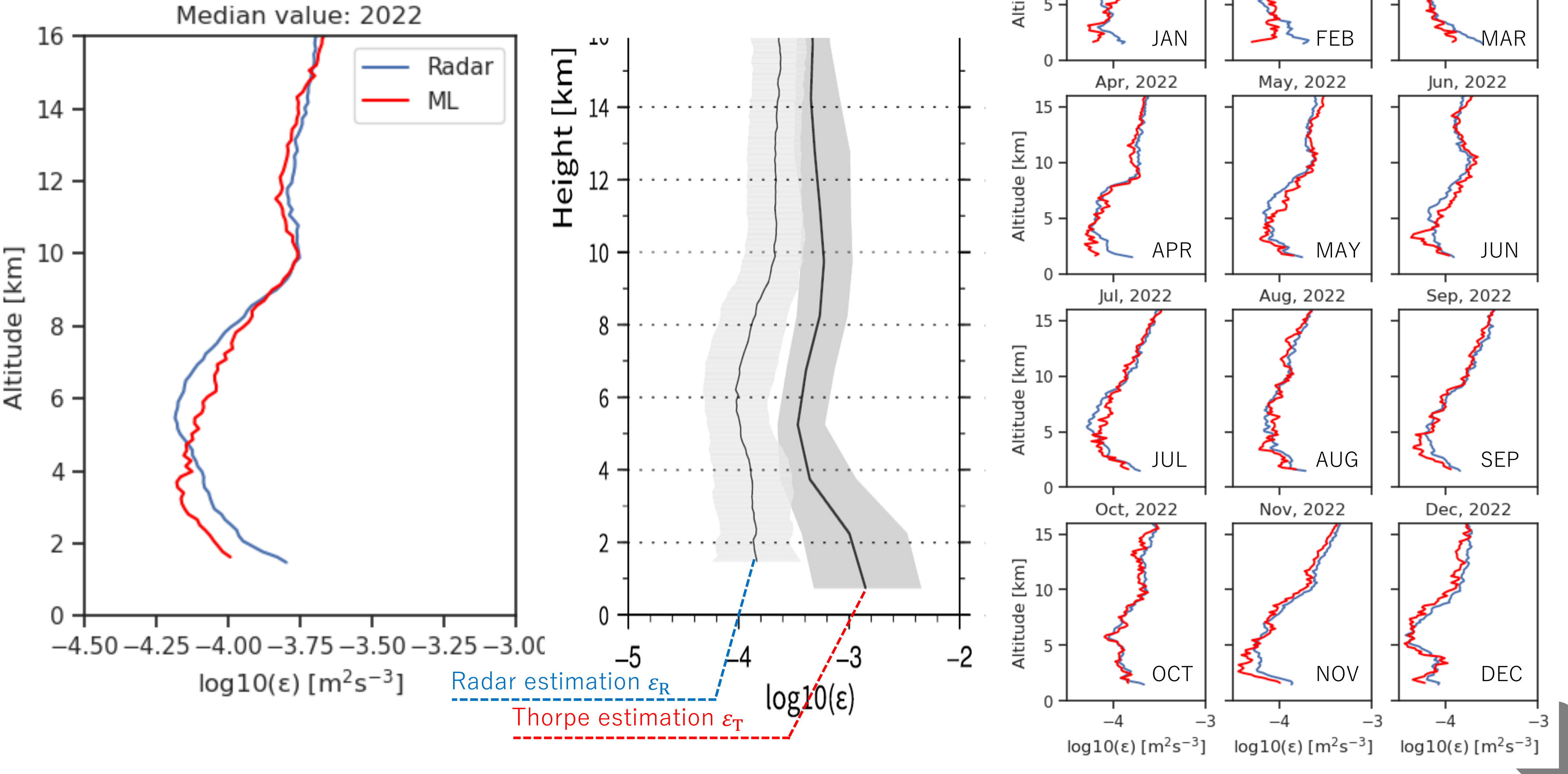

Summary

1. Turbulent Energy Dissipation Rates (ε) Comparison:
   - Used VHF radar data at Syowa Station, Antarctic
   - Compared with radiosonde-based estimation via Thorpe method

   The ratio of radar-based ε to Thorpe-based ε is significantly small in the altitude range of 1.5–9 km compared to over 11 km.

2. Machine Learning (ML) Approach for Estimating ε
   - Developed a ML-based algorithm to estimate ε from the radiosonde observations.

   ML-based estimates closely resemble those obtained from radar observations

   Limitation: The current algorithm fails to detect strong, sporadic turbulence events.
   Applicability to other observation sites?

Prospects

Toward global mapping of turbulent energy dissipation rates

- Improvement the ML-based method
  - Detection of strong turbulence that appears sporadically
  - Validation of the ML-based method using other radars at different latitudes (e.g., MU radar @ Shigaraki, Japan [34.5^{o}N])
    - Generalization ability
    - Assessment of influence of condensation process in the troposphere
- Investigation of which features the ML model is actually looking at to make predictions
- Comparison with other estimation based on observations from aircraft, UAV, special balloon, etc.

Prospects

Toward global mapping of turbulent energy dissipation rates

- Sensitivity test of training data
  - What kind of data (e.g., vertical resolution, θ only, wind only, etc.) are necessary for estimation of ε?
- Another estimation model of radar-based ε (e.g., Luce et al., 2023)
- Application to radiosonde network
  - GRUAN (Global Reference Upper-Air Network) data
    - Well-calibrated data, 30-40 sites
  - BUFR?
    - >1000 sites
    - Various sensors, software versions, vertical resolutions …

GW and turbulence in the mesosphere by the PANSY radar

Sato et al. (2017)： Spectra of winds and momentum fluxes in the summer mesosphere

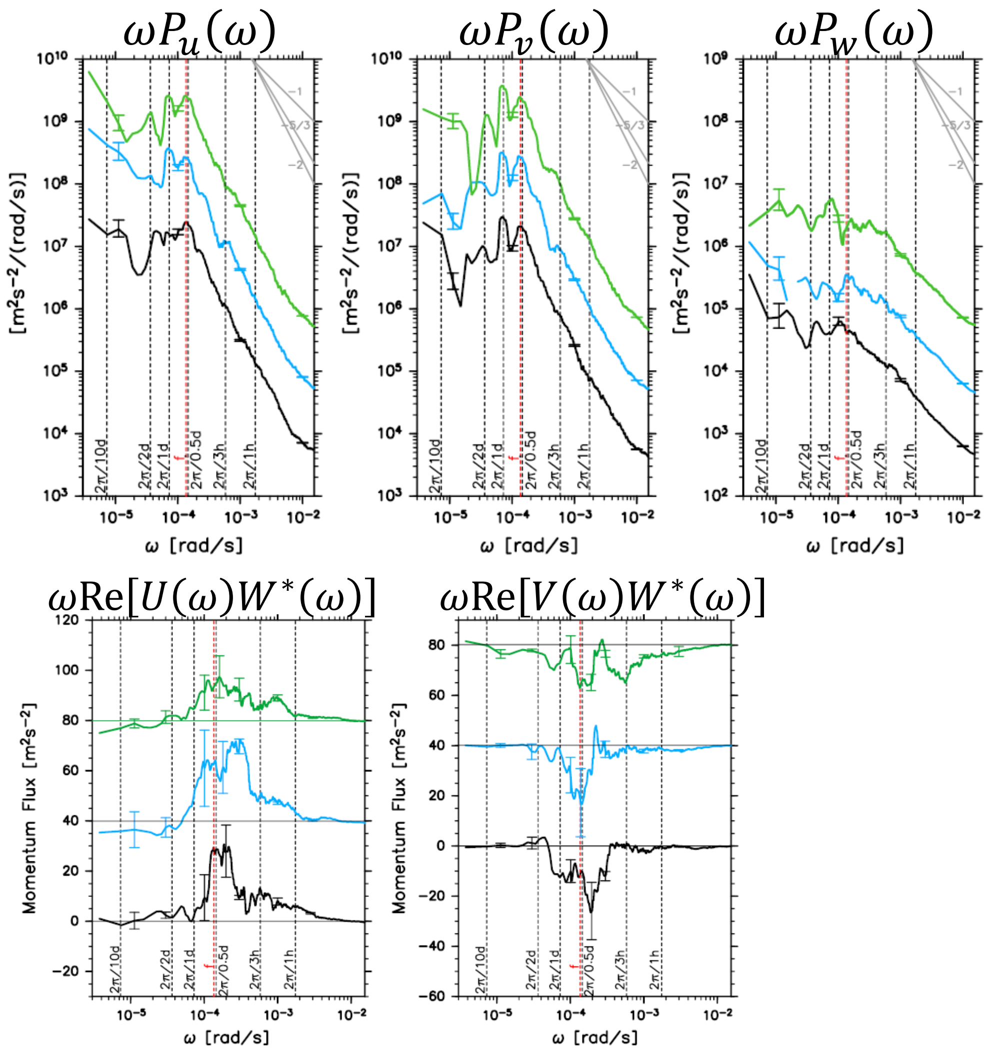

Kohma et al. (2020; 2021)：

Seasonal variation of mesospheric ε

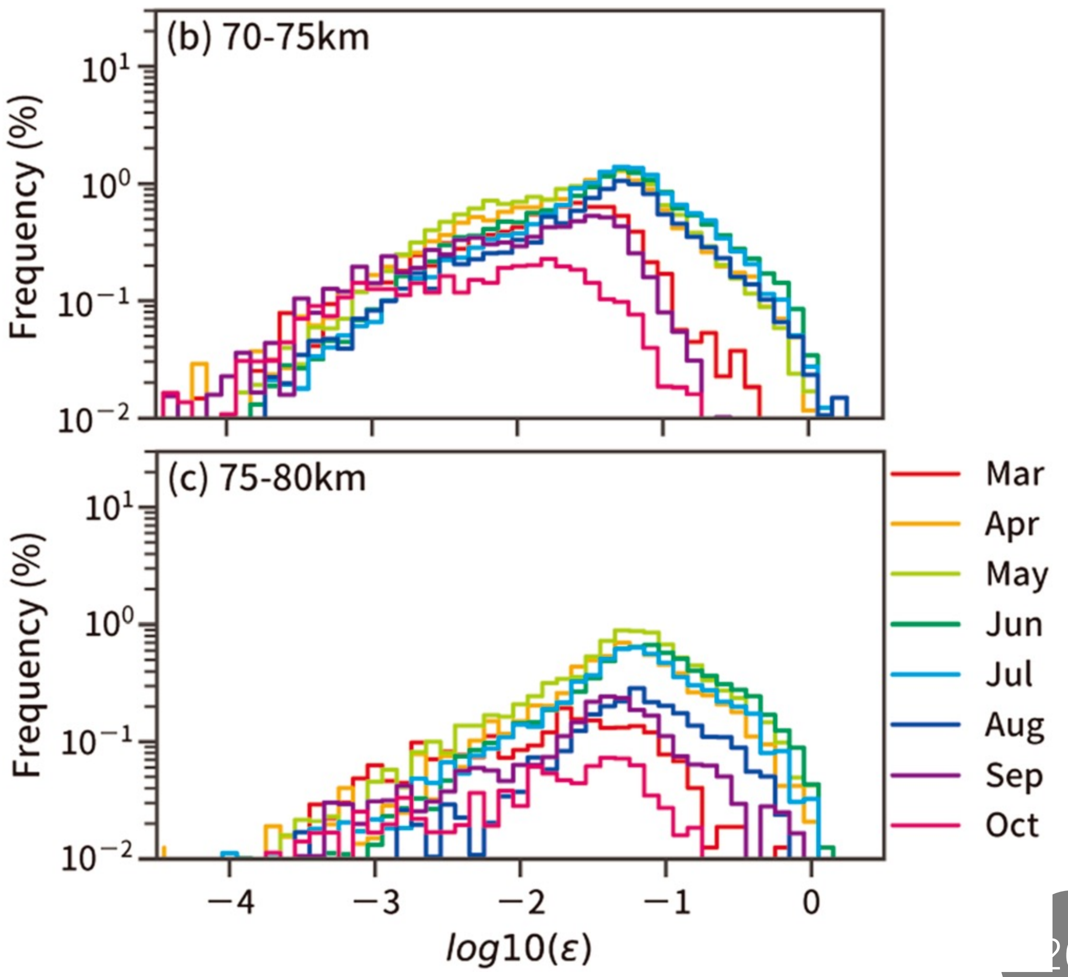

Results: Seasonal variation of ε in 2022

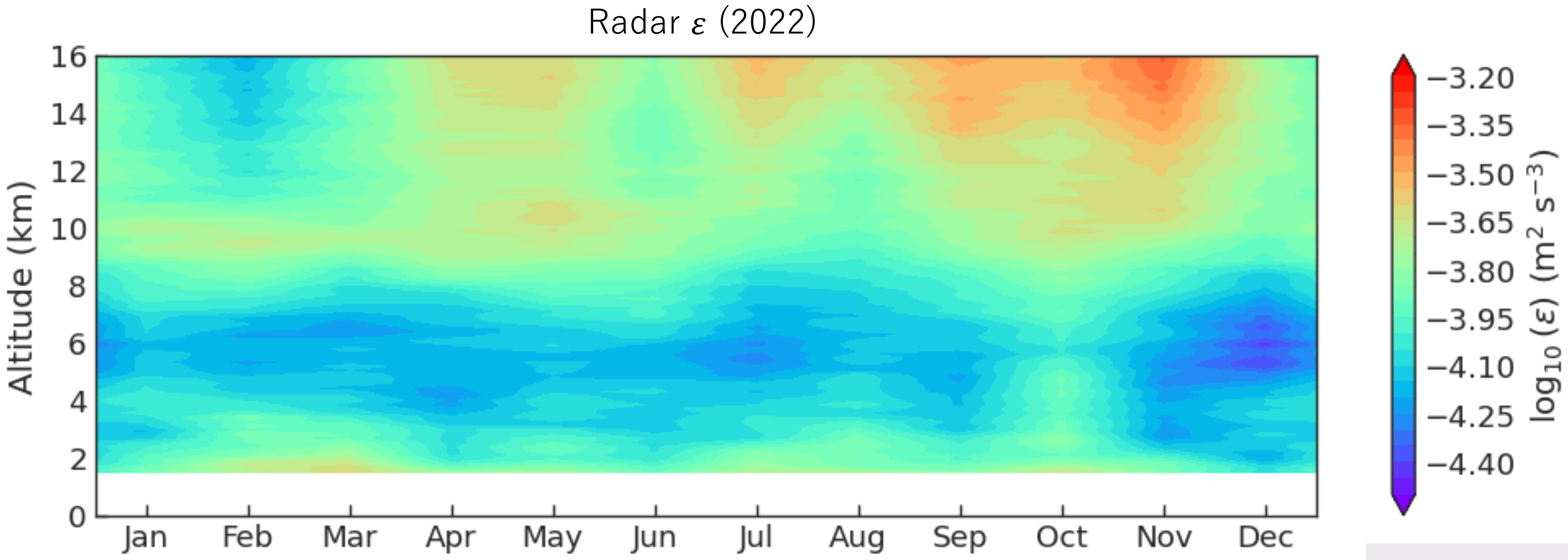

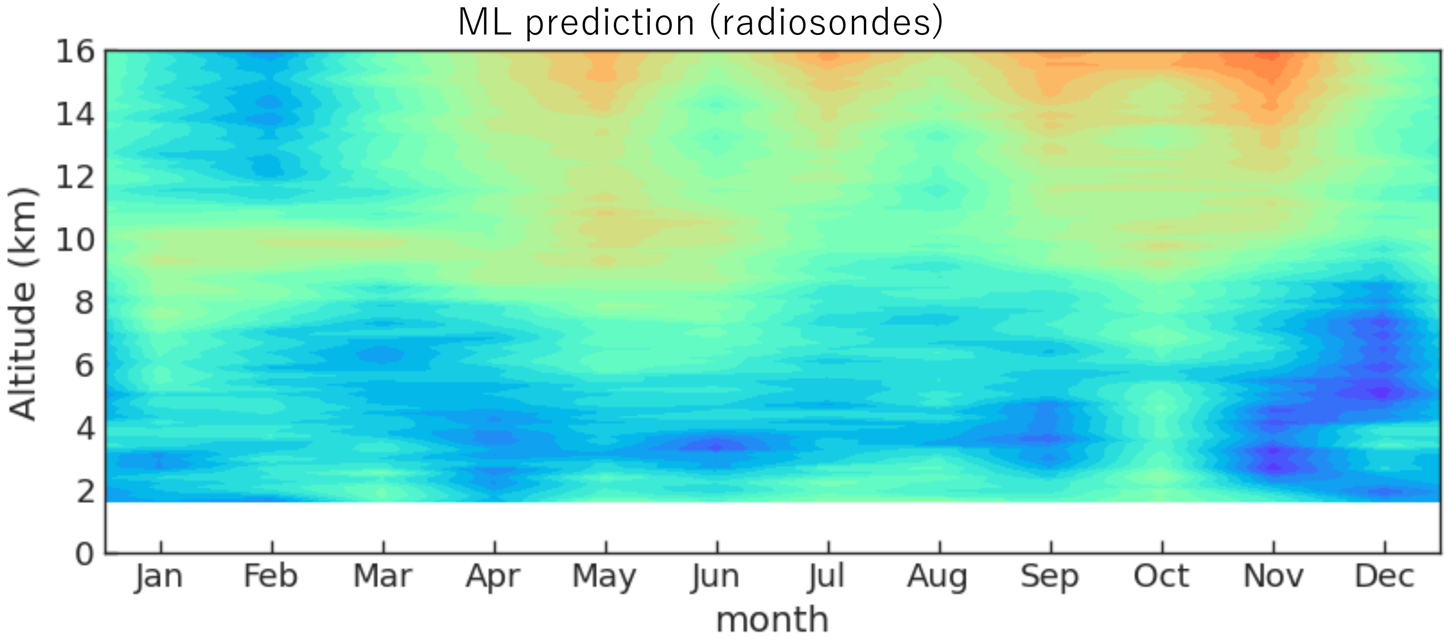

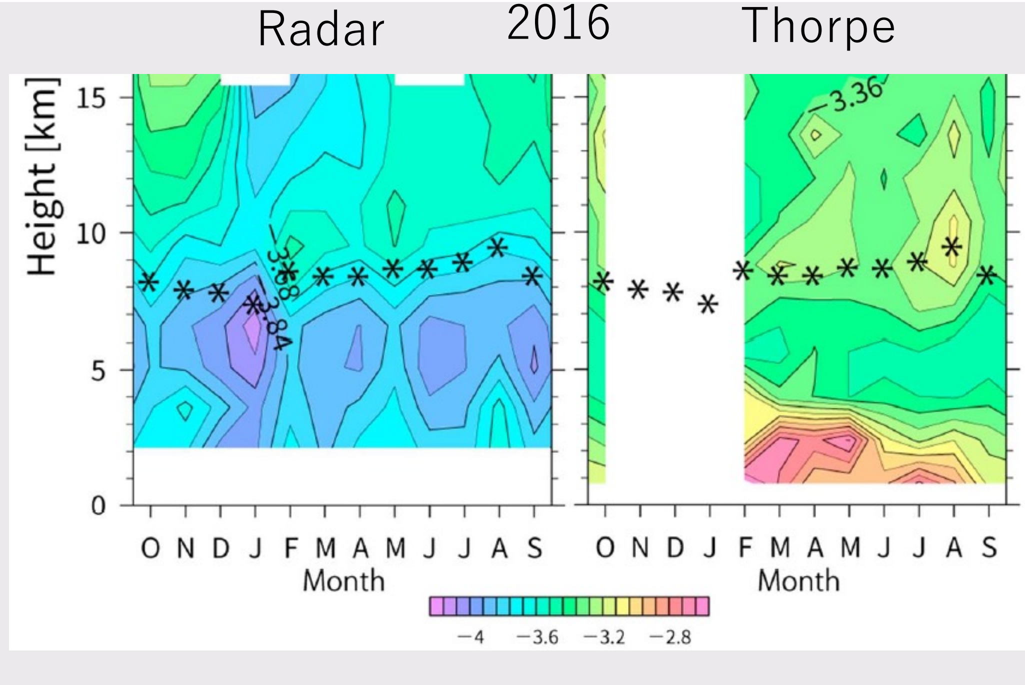

Results: Time-height section of ε in July 2022

ε from the radar

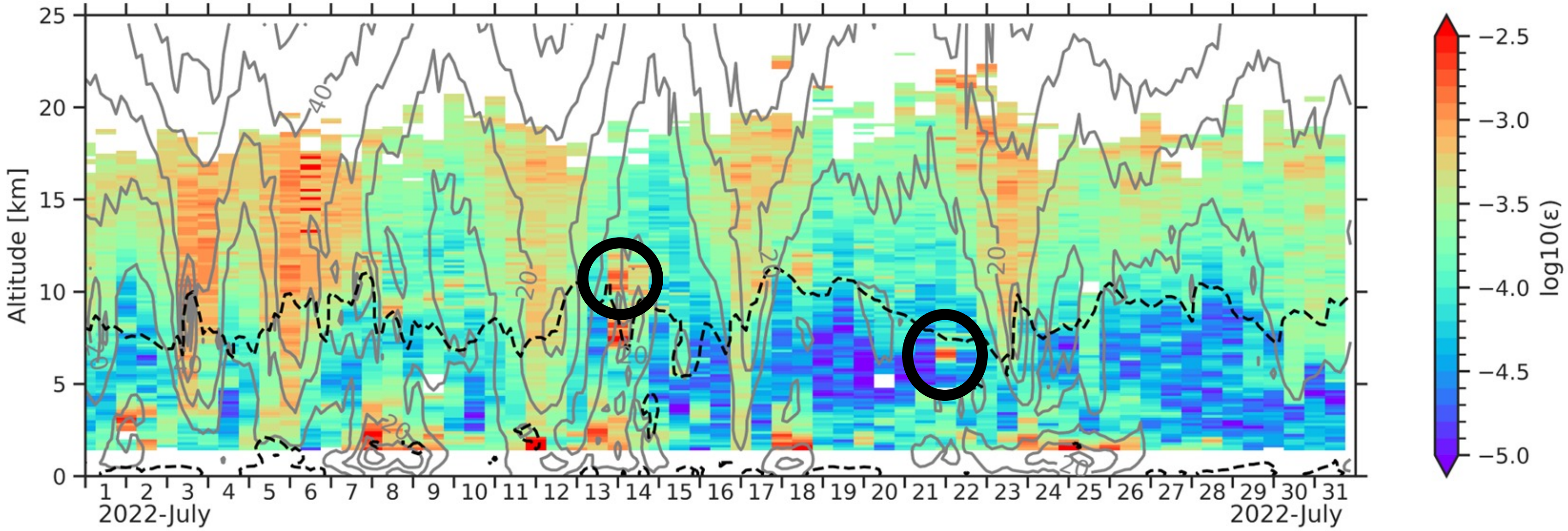

ε from ML-based prediction (radiosondes)

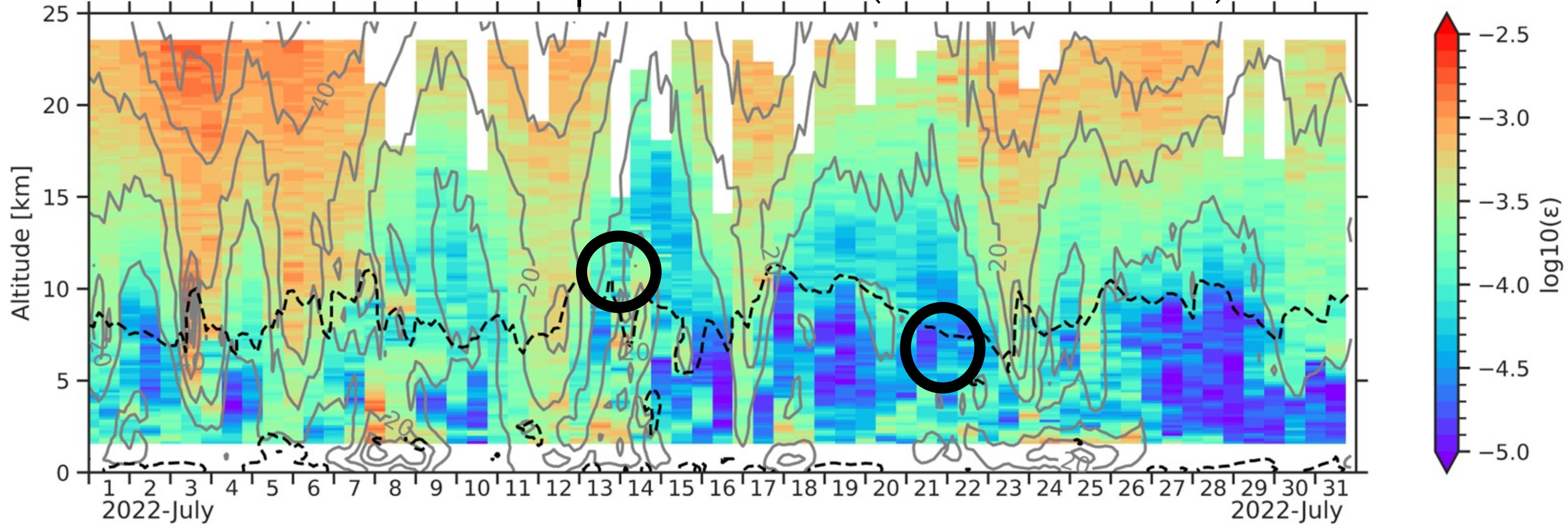

Successful case s

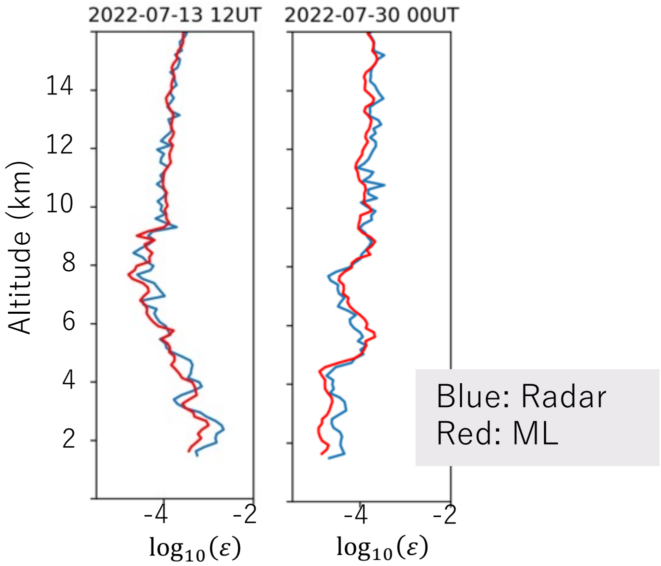

Missing large ε

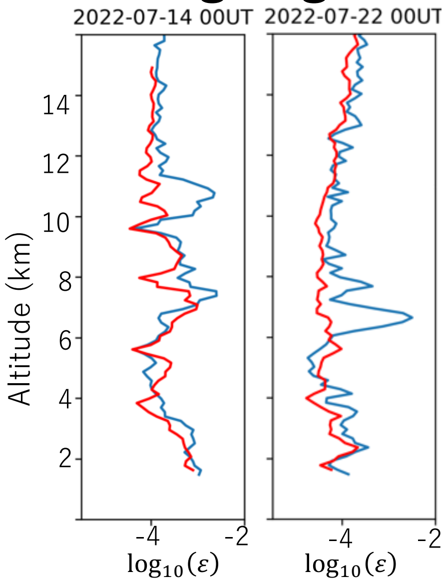

K-H billows observed by PANSY radar

- Minamihara et al. (2023)
  - K-H billow observations using Frequency-domain Interferometric Imaging (FII) techniques
    - FII mode： dt=～13 s, dz=～9.4 m
    - Standard mode： dt=～90 s, dz=～150 m
  - From 10-day continuous observation, 73 K-H billows are detected

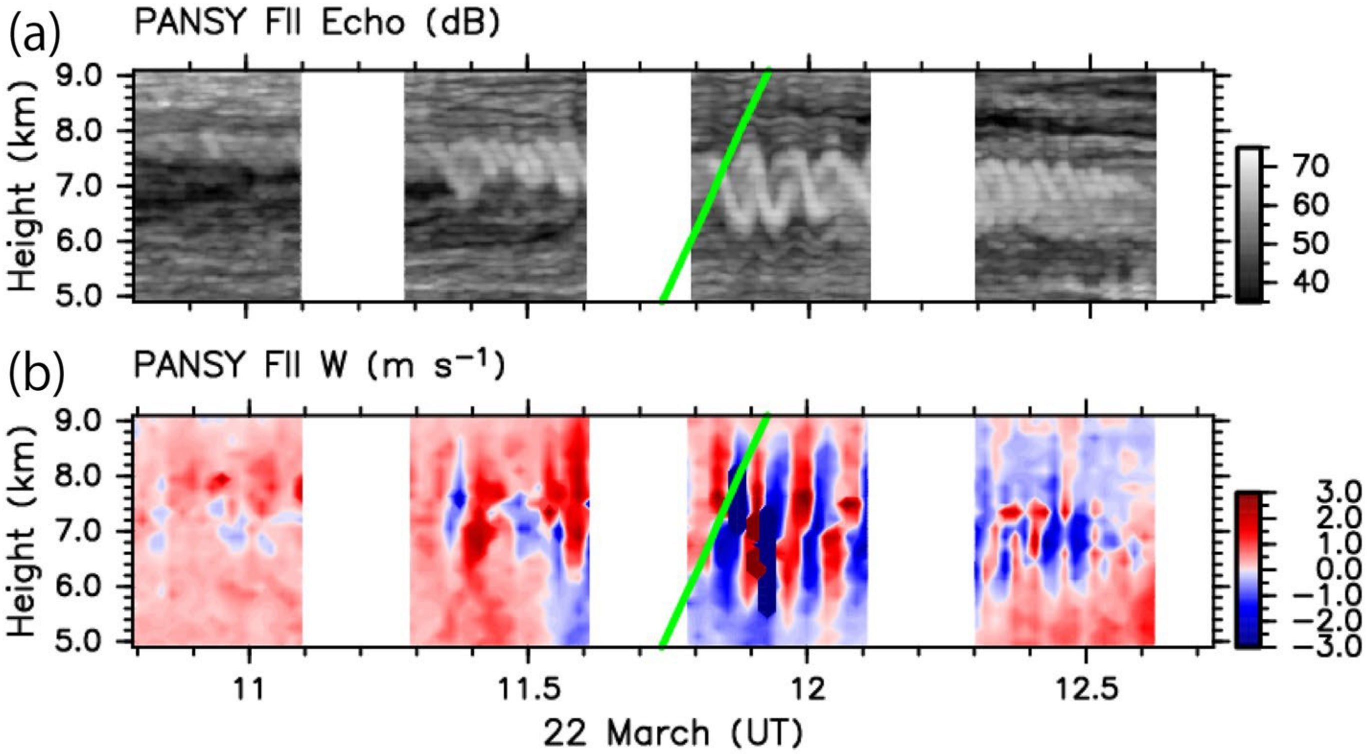

Characteristics of KH billows	PANSY		MU radar[a]	
	Mean	Median	Mean	Median
Depth [m]	559	500	620	550
Wave period [s]	177.6	162.9	90	78
Horizontal wavelength [m]	2,019	1,837	2,600	2,700
Aspect ratio	0.342	0.271	0.22	–
$\log 10\varepsilon_{max}$ [$\mathrm{m\,W\,kg^{-1}}$]	−0.19	−0.22	−0.28	−0.17
Vertical shear [$\mathrm{m\,s^{-1}\,km^{-1}}$]	13.1	12.3	21.4	23.4
Number of samples	73		217	

[a]Fukao et al. (2011).

Results: ML training process and Validation

Loss function (Mean square error)

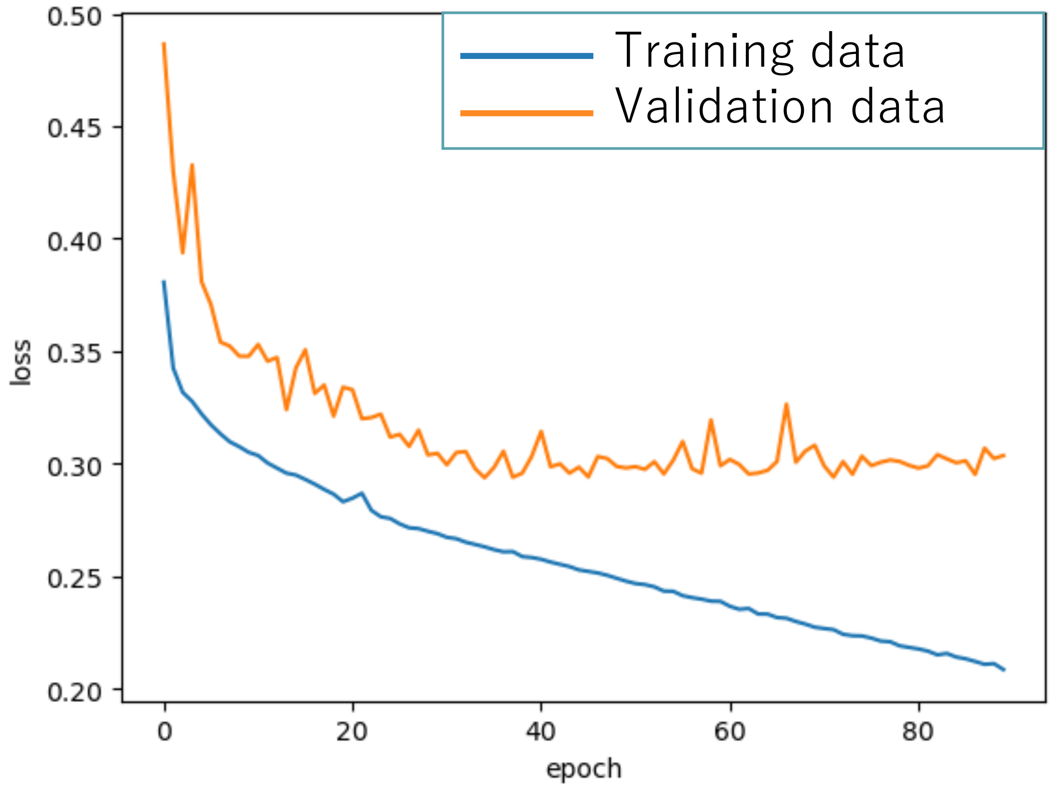

Radar observation vs. ML prediction

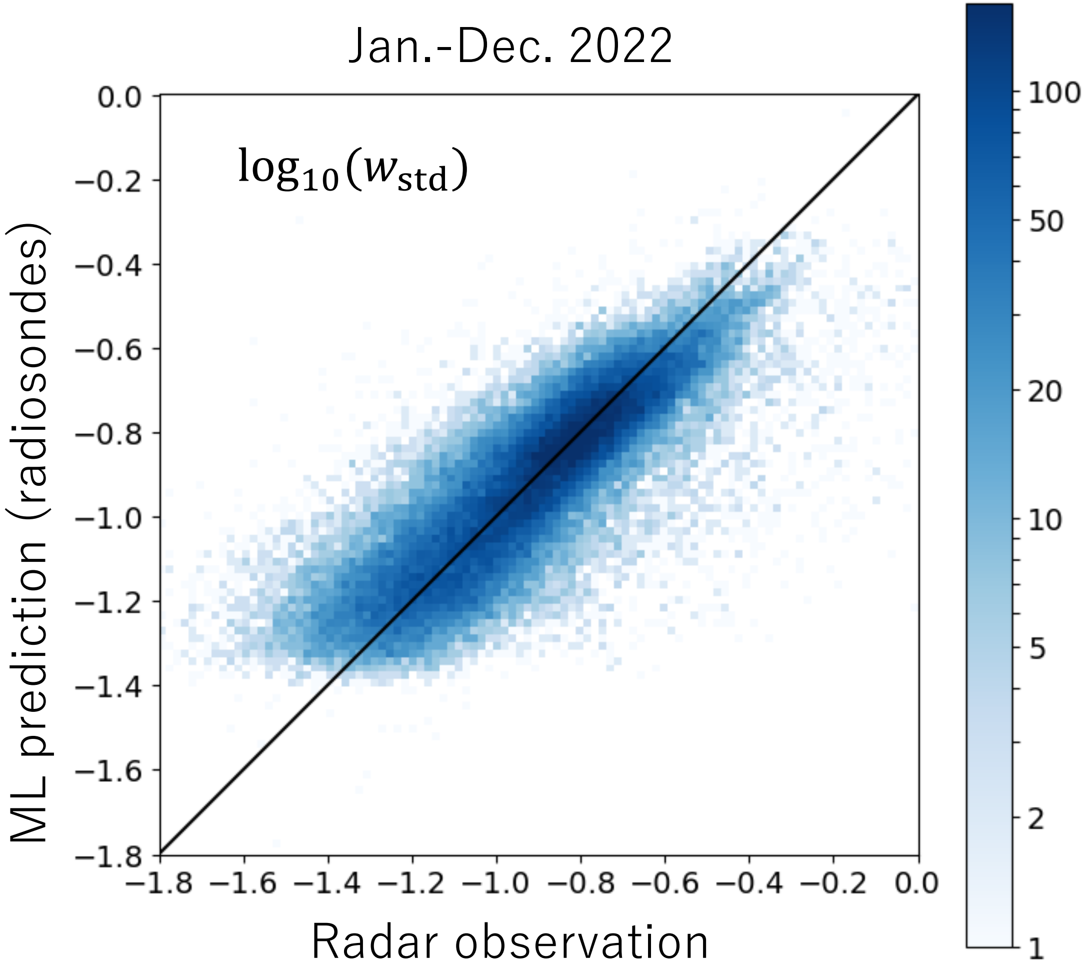

NOTE: Observations in 2022 are not used in the training process

Estimation of the energy dissipation rate using spectral width of backscatter echo of atmospheric radar observations

(Sato and Woodman, 1982; Hocking 1983)

Observed Doppler spectral width (σ_{obs}) of the echo is written as

$$\sigma_{\text{obs}}^2 = \sigma_{\text{T}}^2 + \sigma_{\text{B}}^2 + \sigma_{\text{S}}^2 + \sigma_{\text{W}}^2$$

σ_T^2: Turbulence; σ_B^2: Beam broadening; σ_S^2: Shear broadening; σ_W^2: Time broadening

The turbulent velocity variance (w_{rms}^2) is

$$w_{\text{rms}}^2 = \sigma_T^2/(2\ln 2)$$

Using Kolmogorov spectrum $\mathrm{E}(k) = C\varepsilon^{2/3}k^{-5/3}$

$$\frac{3}{2}w_{\text{rms}}^2 = \int_{k_B}^{k_b} C\,\varepsilon^{2/3}k^{-5/3}dk$$

and assuming $k_B \ll k_b$

$$\varepsilon = C^{-3/2}w_{\text{rms}}^3 k_B$$

Using $k_B = N/\sqrt{w_{\text{rms}}^2}$, $C^{-3/2} \approx 0.5$, and obs. correction

$$\varepsilon = 0.46 N w_{\text{rms}}^2$$

Note: k_B is valid for stably stratified atmosphere

Data: Radiosondes

- Operational radiosonde observations at Syowa Station
  - Meisei RS-06G (**Raw-PTU**), on 00UT and 12UT
  - From Oct. 1, 2015 to Sep. 30, 2016
  - Nighttime data only
  - Interpolated at a constant vertical interval of 12 m from data with 1 second time resolution
  - Potential temperature profiles were reconstructed by replacing the potential temperature with the moist-conservative potential temperature in the cloudy sections (Wilson et al., 2013)
  - Procedure of selection for overturning layers (Wilson et al., 2010; 2011)
- Assuming that $L_T = L_O$ (i.e., $c = 1$), $\varepsilon_{\mathrm{T}} = L_T^2 {N^*}^3$,

where $N^* \equiv \left(\frac{g}{\theta}\frac{\theta_{rms}}{L_{\mathrm{T}}}\right)^{1/2}$ (Bulk buoyancy frequency; Smyth et al., 2001)